ARTICLE

Optical-Limiting Properties of Oleylamine-Capped Gold Nanoparticles for Both Femtosecond and Nanosecond Laser Pulses

Lakshminarayana Polavarapu,[†] N. Venkatram,[‡] Wei Ji,*[,‡] and Qing-Hua Xu*[,†]

Department of Chemistry, National University of Singapore, 3 Science Drive 3, Singapore 117543, Singapore, and Department of Physics, National University of Singapore, 2 Science Drive 3, Singapore 117542, Singapore

ABSTRACT We report strong broad-band optical-limiting properties of oleylamine-capped gold nanoparticles in solution for both femtosecond and nanosecond laser pulses. The nanosecond optical-limiting effects were characterized by using fluence-dependent transmittance measurements with 7 ns laser pulses at 532 and 1064 nm, and the femtosecond optical-limiting effects were characterized with a *z*-scan technique using 300 fs laser pulses at 780 nm. The oleylamine-capped gold nanoparticles were found to show strong broad-band optical-limiting effects for nanosecond laser pulses at 532 and 1064 nm and femtosecond laser pulses at 780 nm. These oleylamine-capped gold nanoparticles displayed exceptional optical-limiting effects with thresholds lower than that of carbon nanotube suspension, a benchmark optical limiter. Input-fluence- and angle-dependent scattering measurements suggested that nonlinear scattering played an important role in the observed optical-limiting behavior at 532 and 1064 nm.

KEYWORDS: gold nanoparticles • optical limiting • plasmon resonance • nonlinear optical properties • *z*-scan • femtosecond laser

INTRODUCTION

Optical limiters display a decreasing transmittance as a function of laser fluence or irradiance. Fast-response optical-limiting materials with low thresholds can be used for the protection of eyes and sensitive optical devices from laser-induced damage. A lot of efforts have been devoted to developing ideal broad-band optical-limiting materials based on mechanisms such as nonlinear scattering (1), multiphoton absorption (2), and reverse saturable absorption (3, 4). Strong optical-limiting properties have been observed in various materials such as carbon nanotubes (CNTs) (1, 5, 6) and carbon-black suspensions (7), metallophthalocyanines (8), and porphyrins (9). Inorganic nanomaterials provide an attractive alternative to organic materials for various photonic applications because of their stability and simple synthetic methods. Metal nanoparticles, such as gold and silver nanoparticles, have recently been found to exhibit strong optical-limiting properties (3, 4, 10−18). The development of optical-limiting materials using metal nanoparticles is attractive because gold and silver nanoparticles are easy to prepare, highly soluble, and stable in both aqueous and organic solvents.

So far, there are only a few reports on the optical-limiting properties of gold and silver nanocomposites. Goodson et al. (11) reported a strong optical-limiting performance in metal−dendrimer nanocomposites with the nanosecond laser pulses. Philip et al. (13) reported optical-limiting effects in monolayer-protected gold nanoparticles with picosecond laser pulses. The optical-limiting properties of metal nanoparticles depend on the size of the nanoparticles and their surrounding matrix (14) or the solvent in which the nanoparticles are dissolved (6). Francois et al. (19) studied the effect of the particle size on the optical-limiting behavior of gold nanoparticles at 530 nm using picosecond laser pulses. They have observed that the threshold of the optical-limiting effect decreased with increasing particle size because of nonlinear scattering. Wang and Sun (17) investigated the optical-limiting properties of citrate-stabilized gold nanoparticles and their aggregates. They found that aggregated gold nanoparticles showed strong optical-limiting properties even though individual gold nanoparticles exhibited no optical-limiting behavior. Very recently, we have reported strong optical-limiting effects of silver nanotriangles with a threshold comparable to that of benchmark CNTs (4). The applications of CNTs are limited by their poor solubility in aqueous and organic solvents and strong tendency to aggregate quickly (20). Noble-metal nanoparticles are a good alternative to CNTs because noble metals are stable and can be easily well dispersed in aqueous and organic solvents. Most of the above-mentioned studies on the optical-limiting properties of metal nanoparticles were performed with nanosecond laser pulses with a central wavelength of 532 nm. There are very few reports on the ultrafast optical limiting using noble-metal nanoparticles (3, 21). Previously, Scalora et al. (22) reported optical limiting and switching of ultrashort

* E-mail: chmxqh@nus.edu.sg (Q.-H.X.), phyjiwei@nus.edu.sg (W.J.).
Received for review June 27, 2009 and accepted August 31, 2009
[†] Department of Chemistry.
[‡] Department of Physics.
DOI: 10.1021/am900442u

Published on Web 09/18/2009

pulses in photonic band-gap materials. Nanomaterials with optical-limiting properties for the near-IR or femtosecond laser pulses have been less stduied (3, 4, 23, 24).

In this work, we have prepared oleylamine-capped gold nanoparticles in toluene and studied their optical-limiting response to the laser pulses. The optical-limiting properties of those gold nanoparticles were characterized by fluence-dependent transmittance measurements using 532 and 1064 nm laser pulses with a pulse duration of ~7 ns. Their femtosecond optical-limiting properties were studied by performing a *z*-scan experiment with 780 nm femtosecond laser pulses with a pulse duration of 300 fs. The oleylamine-capped gold nanoparticles were found to show strong broadband optical-limiting effects for nanosecond laser pulses at 532 and 1064 nm and femtosecond laser pulses at 780 nm.

EXPERIMENTAL SECTION

Materials. Gold chloride trihydrate ($HAuCl_4 \cdot 3H_2O$), oleylamine, oleic acid, and ascorbic acid were purchased from Sigma-Aldrich. Toluene was purchased from Merck. All of the materials were used as received without further purification.

Synthesis of Oleylamine-Capped Gold Nanoparticles. In a typical synthesis of gold nanoparticles, 100 μL of water was added to 30 mg of solid chloroauric acid. The solution was then mixed with 50 mL of toluene containing 400 μL of oleylamine and 200 μL of oleic acid. The obtained yellow solution was refluxed at 100 °C. The solution turned to colorless within 15 min. The heating of the solution was stopped upon the color change, and the solution was aged for 12 h until the color eventually changed into pink. A total of 40 mg of ascorbic acid (in 25 mL of toluene) was then added into the pinkish solution. After aging for 24 h, the solution changed to a dark red. The solution was centrifuged with a speed of 10 000 rpm for 1 h, and the precipitate was dispersed in toluene. Transmission electron microscopy (TEM) images of the obtained gold nanoparticles were taken from a Philips CM10 electron microscope at an accelerating voltage of 100 kV.

Fourier Tranform IR (FTIR) Measurement of the Oleylamine-Capped Gold Nanoparticles. The IR spectra were measured by using a Biorad Excalibur FTIR spectrometer. The oleylamine-capped gold nanoparticles were centrifuged four times to fully remove the uncapped oleylamine molecules. The precipitate was dissolved in chloroform, and a drop of solution was cast onto the NaCl substrate for FTIR measurements.

Optical-Limiting Measurements. The optical-limiting properties of the gold nanoparticles at 532 and 1064 nm were characterized by fluence-dependent transmittance measurements with 532 and 1064 nm laser pulses with a pulse duration of 7 ns. The laser pulses were generated from a Q-switched Nd:YAG (yttrium–aluminum–garnet) laser (Spectra Physics DCR3). The primary laser output had a center wavelength of 1064 nm, with a pulse duration of 7 ns and a repetition rate of 10 Hz. The 1064 nm output was frequency-doubled to obtain 532 nm laser pulses. The laser beam was focused onto the gold nanoparticle solution contained in a 1-cm-path-length quartz cuvette with a spot size of 165 μm. The nanoparticle solution was stirred to refresh the samples at the laser illumination spot to minimize potential thermal or photoinduced shape transformation. To understand the mechanisms of the optical-limiting effects, the scattered light signal around the sample was collected at different angles from the laser focus.

The optical-limiting properties at 780 nm were measured by using a femtosecond *z*-scan technique. The femtosecond laser pulses were generated by a mode-locked Ti:sapphire laser (Quantronix, IMRA), which seeded a Ti:sapphire regenerative amplifier (Quantronix, Titan) with a pulse duration of 300 fs.

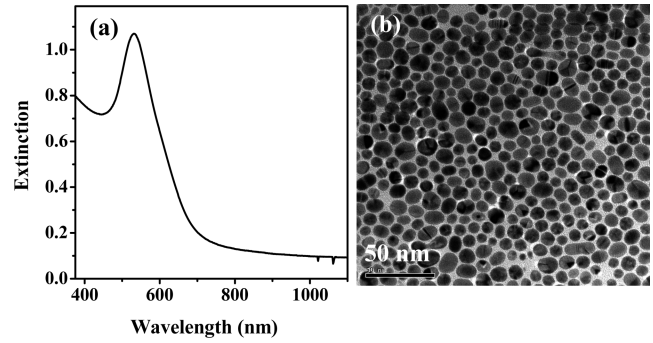

FIGURE 1. UV–visible spectrum (a) of an oleylamine-capped gold nanoparticle solution and its corresponding TEM image (b). The scale bar is 50 nm.

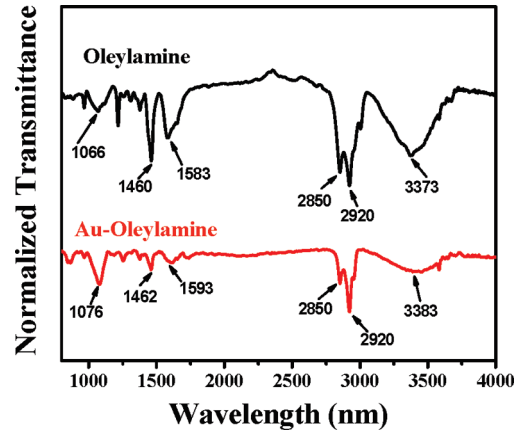

FIGURE 2. FTIR spectra of oleylamine and oleylamine-capped gold nanoparticles.

The laser pulses were focused onto the gold nanoparticle solution in a 1-mm-path-length quartz cuvette, with a beam waist of ~30 μm. The solution had a linear transmittance of 80%. The incident and transmitted laser powers were monitored as the cuvette moved along the *z* direction, toward and away from the focus position.

RESULTS AND DISCUSSION

In a typical synthesis, oleylamine-capped gold nanoparticles were prepared using a procedure modified from the one reported by Halder and Ravishankar (25), in which oleylamine and oleic acid were used as capping agents to prepare thin nanowires. In our experiments, we found that the concentration of $HAuCl_4$ played a very important role in the morphology of the obtained gold nanostructures. By using a low concentration of $HAuCl_4$ in the reaction, spherical gold nanoparticles instead of gold nanowires were obtained. Figure 1 shows the UV–visible extinction spectrum of the gold nanoparticles in toluene and the corresponding TEM image. The UV–visible spectrum of the gold nanoparticles in toluene has an extinction maximum at 535 nm with a tail stretching into longer-wavelength regions up to near-IR. The size of the obtained gold nanoparticles was in the range of 7–10 nm with an overall spherical shape, together with some larger particles with various nonspherical shapes.

Figure 2 shows the FTIR spectrum of pure oleylamine and oleylamine-capped gold nanoparticles. The IR spectrum of oleylamine is similar to that previously reported (26). The oleylamine-capped gold nanoparticles have spectral signa-

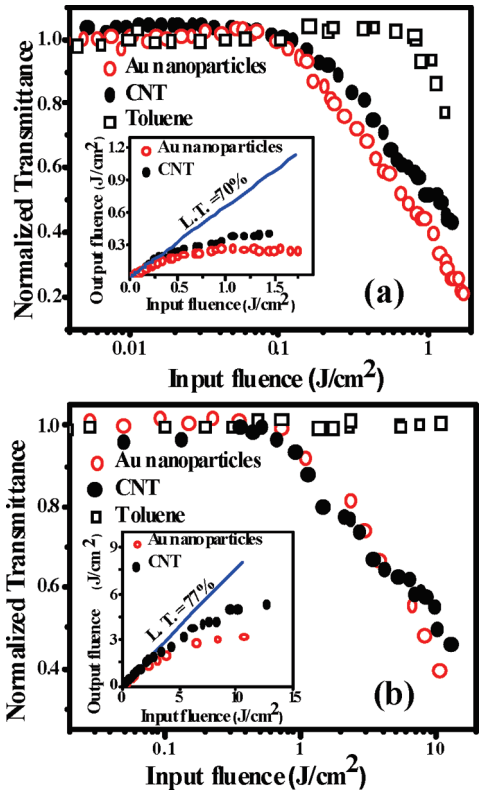

FIGURE 3. Optical-limiting response of an oleylamine-capped gold nanoparticle solution, CNT suspension, and toluene measured using 7 ns laser pulses at 532 nm (a) and 1064 nm (b). The insets show the corresponding output energy density (J/cm^2) as a function of the input energy density (J/cm^2).

tures similar to those of pure oleylamine. Several bands are slightly shifted because of the surface effect of gold nanoparticles when oleylamine is capped onto the gold nanoparticles. For example, the band at 3373 cm^{-1} in the IR spectrum of oleylamine is due to the N−H stretching mode, which is red-shifted to 3383 cm^{-1} for oleylamine-capped gold nanoparticles. There is no shift for the C−H stretching band around 2850−2920 cm^{-1} after oleylamine is bound to the nanoparticle. The bands at 1066 and 1460 cm^{-1} are attributed to the ═C−H and −C−H bending modes in oleylamine, respectively, which were shifted to 1076 and 1462 cm^{-1} in oleylamine-capped gold nanoparticles. The band at 1583 cm^{-1} in oleylamine is due to the N−H bending mode, which is shifted to 1593 cm^{-1} in the oleylamine-capped gold nanoparticles.

Figure 3 displays the nonlinear transmittance of the oleylamine-capped gold nanoparticles in toluene with 7 ns pulses at 532 nm (Figure 3a) and 1064 nm (Figure 3b). The insets are the corresponding plots of the output energy density (J/cm^2) as a function of the input energy density. The linear transmittances of the nanoparticles at 532 and 1064 nm were adjusted to 70% and 77%, respectively. CNTs have been known as a benchmark optical-limiting material (1), and its optical-limiting property was also characterized under the same experimental conditions and with the same linear transmittance as that of oleylamine-capped gold nanoparticles for direct comparison. It has been previously reported that toluene showed slight optical-limiting activity at 532 nm (13). The optical-limiting property of pure toluene was also measured at the same conditions to clarify the solvent contribution.

As shown in Figure 3a, the transmittance of an oleylamine-capped gold nanoparticle solution slightly increases as the input energy density increases up to 0.07 J/cm^2, which was believed to be due to saturable absorption of the nanoparticles (4). Saturable absorption of nanoparticles arises from ground-state plasmon bleaching at moderate intensities, which results in the reduction of light absorptivity of materials with increasing light intensity. When the input fluence further increases, the transmittance starts to decrease, displaying optical-limiting activity. The optical-limiting performance of these oleylamine-capped gold nanoparticles is even better than that of CNTs, a benchmark optical-limiting material. The limiting threshold is defined as the incident fluence at which the transmittance falls to 50% of the normalized linear transmittance (1). The limiting thresholds at 532 nm are 0.6 and 1.0 J/cm^2 for the oleylamine-capped gold nanoparticles and CNTs, respectively. In the pure toluene, we also observed an optical-limiting effect at 532 nm with a threshold much higher than that of the oleylamine-capped gold nanoparticles in toluene. These results suggest that the major contribution arises from the gold nanoparticles. The limiting threshold for these oleylamine-capped gold nanoparticles is significantly better than those previously reported for monolayer-protected gold nanoparticles (13), dendrimer-capped gold nanoparticles (11), and covalently bonded gold nanoparticles (15). In these previous studies, the threshold of these materials has been reported to be ~2 J/cm^2.

Figure 3b shows the optical-limiting properties of an oleylamine-capped gold nanoparticle solution, CNT suspension, and toluene at 1064 nm. The optical-limiting performance of the gold nanoparticles at 1064 nm was found to be slightly better than that of CNTs, while no optical-limiting effect was observed in the toluene solvent at 1064 nm. The limiting thresholds for the gold nanoparticles and CNTs at 1064 nm are 7.5 and 10.0 J/cm^2, respectively.

The femtosecond optical-limiting properties of the oleylamine-capped gold nanoparticles in toluene were characterized by using a femtosecond *z*-scan technique using 300 fs laser pulses at 780 nm. Figure 4a shows the open-aperture *z*-scan measurement at two input intensities. In a *z*-scan experiment, the pump density increases as the sample moves into the beam focus. The *z*-scan measurements on the gold metal nanoparticle solution at both input intensities show a reverse saturable absorption behavior: the transmission of the sample decreases as the sample moves into the beam focus. The observed reverse saturable absorption is an indicator of the optical-limiting effect. The optical-limiting effect can be manifested by plotting the output energy density versus the input energy density as shown in Figure 4b (the data were extracted from the open-aperture *z*-scan measurements). The sample exhibits high linear transmittance (85%) at lower input fluence, and the transmittance decreases as the input fluence exceeds 8 J/cm^2, displaying

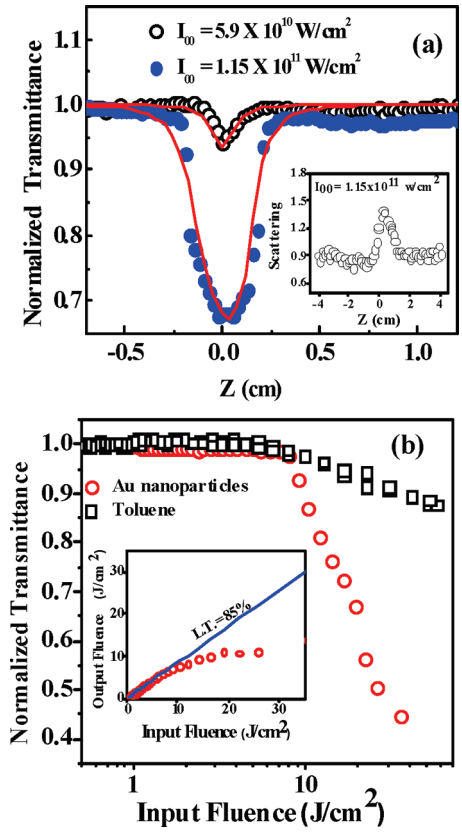

FIGURE 4. (a) Typical open-aperture *z*-scan measurement for an oleylamine-capped gold nanoparticle solution at 780 nm with a pulse width of 300 fs at two different input intensities. The inset shows the results of scattering experiments obtained by placing a detector at an angle of 45° to the laser beam direction during the *z*-scan experiments. (b) Optical-limiting behavior of an oleylamine-capped gold nanoparticle solution and pure toluene at 780 nm. The data were extracted from the *z*-scan measurements. The inset of part b shows the output fluence (J/cm^2) as a function of the input fluence (J/cm^2) for an oleylamine-capped gold nanoparticle solution.

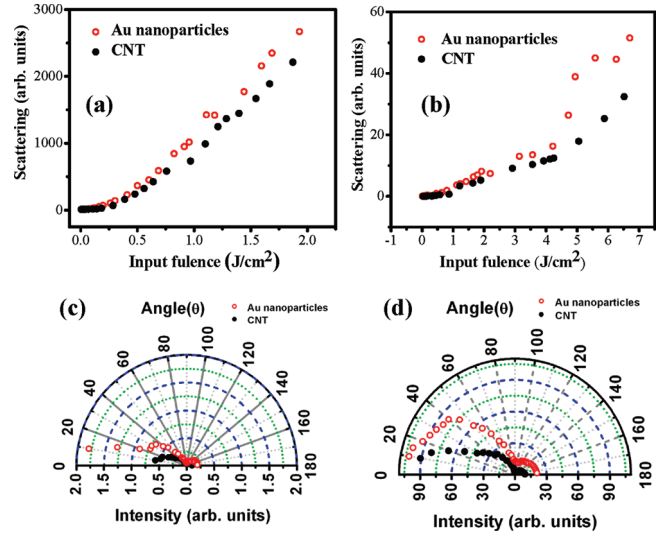

FIGURE 5. Nonlinear scattering results for the oleylamine-capped gold nanoparticle solution and CNT suspension using 532 nm (7 ns) (a and c) and 1064 nm (7 ns) (b and d) laser pulses. (a and b) Nonlinear scattering signals at an angle of 40° to the propagation axis of the transmitted laser beam. (c and d) Polar plot of the scattering signal as a function of the angular position of the detector for oleylamine-capped gold nanoparticles (c) and CNTs (d).

an optical-limiting activity with a threshold of 26.0 J/cm^2. We have also measured the nonlinear transmission of pure toluene under the same experimental conditions. Pure toluene was found to show much lower nonlinearity compared to that of an oleylamine-capped gold nanoparticle solution, suggesting that the major contribution arises from the gold nanoparticles.

Several mechanisms, such as multiphoton absorption (27) and nonlinear scattering (1, 4), could be responsible for the optical-limiting activity of the materials. We have recently demonstrated that the optical-limiting property of metal nanoparticles at 532 nm was mainly due to nonlinear scattering (4, 12). To understand the mechanisms responsible for the strong optical-limiting activity of these oleylamine-capped gold nanoparticles at 532 and 1064 nm, we have also performed input-fluence-dependent scattering experiments on an oleylamine-capped gold nanoparticle solution and CNT suspension using 532 and 1064 nm laser pulses (Figure 5). The scattering signals were monitored at different angles to the propagation axis of the transmitted laser beam. Parts a and b of Figure 5 show the input-laser-fluence-dependent scattering signal collected at an angle of 40° to the propagation axis of the transmitted laser beam at 532 and 1064 nm. For both the oleylamine-capped gold nanoparticle solution and CNT suspension samples, the scattering signals were dominated by linear scattering at low input fluences and became deviated from linear behavior as the input fluence increased above some threshold. The contribution from nonlinear scattering became the dominant contribution at high pump fluences. Parts c and d of Figure 5 show the scattering signals at different angles (every 5° from 10 to 180°) with respect to the transmitted laser beam for both the oleylamine-capped gold nanoparticle solution and CNT suspension with an incident intensity of 1.5 J/cm^2 for 532 nm laser pulses and 5 J/cm^2 for 1064 nm laser pulses. For both gold nanoparticles and CNTs, the scattering signals in the forward directions were significantly larger than those in the backward directions. The light-scattering signals of the gold nanoparticles were significantly larger than those of CNTs in both the forward and backward directions at both 532 and 1064 nm. For the 532 nm laser pulses, the larger difference between the scattering signals of gold nanoparticles and CNTs occurred at smaller angles (<20°). In the case of 1064 nm laser pulses, the larger difference in the scattering signals of gold nanoparticles and CNTs occurred at ~40°. These results suggest that the nonlinear scattering played an important role in the observed optical-limiting activity. The magnitude of the scattered signal for the oleylamine-capped gold nanoparticles is higher than the scattering signal from CNTs at both 532 and 1064 nm, consistent with the better optical-limiting performance of the oleylamine-capped gold nanoparticles compared to CNTs.

The nonlinear scattering usually arises from the formation of two types of scattering centers after photoexcitation of the nanoparticles. At higher pump fluence, the excitation energy absorbed by the nanoparticle creates a fast expansion of the metal nanoparticle, which acts as a scattering

center. The absorbed energy is subsequently transferred to the surrounding solvent. Consequently, the solvent is heated up and the bubbles are formed, which act as the secondary scattering centers (10). The solvent in which nanoparticles are dispersed plays an important role in enhancing the optical-limiting activity of the nanoparticles through microbubble formation. Microbubble formation usually occurs at the interface of the solvent and nanoparticle. Solvents with good thermal conductivity can quickly transfer the thermal energy from the nanoparticle to the solvent after photoexcitation to dissipate the energy. Solvents with low thermal conductivity can help to confine the energy at the interface and promote the solvent vaporization and bubble formation. Nanoparticles dispersed in solvents with low thermal conductivity, low heat capacity, and low boiling point are expected to show a good performance in generating scattering centers and hence give rise to optical-limiting effects. It has been recently reported by Wang and Blau that the optical-limiting properties of CNTs are better in low-boiling solvents (6).

We have compared the optical-limiting performance of the oleylamine-capped gold nanoparticles in toluene with the citrate-capped gold nanoparticles in water at the same experimental conditions. The citrate-capped gold nanoparticles did not show any optical-limiting activity (see the Supporting Information). The boiling points of water and toluene are quite similar. However, the thermal conductivity and heat capacity of toluene are much lower than those of water. In addition, in the oleylamine-capped gold nanoparticles, gold is passivated through the −NH group with the oleylamine ligand. It has been previously demonstrated that the metal-to-solvent energy transfer is faster in amine (NH)- and thiol (SH)-passivated gold nanoparticles compared to that in the citrate-capped gold nanoparticles (28−30). The optical-limiting activity in NH- and SH-passivated gold nanoparticles has been previously reported by a few groups (11, 13). Therefore, fast metal-to-solvent energy transfer, low thermal conductivity, and low heat capacity all contribute together, leading to a quick local heating of the interface layer between the particle and solvent, which raises the temperature above a critical temperature to form the bubbles. These microbubbles act as scattering centers and result in enhanced optical-limiting properties in oleylamine-capped gold nanoparticles in toluene, compared to citrate-capped gold nanoparticles in water.

The reverse saturable absorption of gold nanoparticles under the illumination of femtosecond laser pulses at 780 nm was usually believed to be due to nonlinear absorption, including excited-state absorption (3, 31, 32) and plasmon-enhanced multiphoton absorption (33, 34). The excited-state absorption includes photothermally induced transient absorption (31, 32) and free carrier absorption (3). Upon photoexcitation, the electrons are excited to energy levels higher than the Fermi level, resulting in an increased electronic temperature. The increase in the electronic temperature will lead to new transient absorption signals (31, 32). However, we have also performed *z*-scan measurements for the citrate-capped gold nanoparticles in water under the same experimental conditions. Saturable absorption, instead of the optical-limiting effect, was observed for the citrate-capped gold nanoparticles (see Figure S4 in the Supporting Information). The results suggest that the nonlinear absorption should not be the dominant factor that accounts for the reverse saturable absorption observed for the oleylamine-capped gold nanoparticles because nonlinear absorption should apply similarly for gold nanoparticles dispersed in toluene and water. Considering that the major difference between the two systems is the solvent, nonlinear scattering should play a very important role for the observed optical-limiting effect for femtosecond pulses at 780 nm. The scattering centers are formed mainly because of the thermally induced nonlinearity. We have performed scattering experiments for both oleylamine-capped gold nanoparticles in toluene and citrate-capped gold nanoparticles in water under the same experimental conditions, by placing a detector at an angle of 45° to the laser beam direction during the *z*-scan experiments. In the case of oleylamine-capped gold nanoparticles in toluene, the scattering intensity increased as the sample moved toward the focus of the laser beam (see the inset of Figure 4a). There was nearly no increase in the scattering signal for the citrate-capped gold nanoparticles (see the inset of Figure S4 in the Supporting Information) under the same experimental conditions. These results suggest that nonlinear scattering plays a very important role in the optical nonlinearity of the oleylamine-capped gold nanoparticles.

The *z*-scan results can be fitted well by considering both linear absorption, two-photon absorption, and scattering (linear and nonlinear) as shown in Figure 3a by using the equation (35, 36)

$$\frac{dI}{dz} = -\alpha_0 I - \beta I^2 - \alpha_s I \qquad (1)$$

where $\alpha_s = g_s(\Delta\tilde{n})^2 \approx g_s(\Delta n_0 + \Delta n_2 I)^2$, α_0 is the ground-state absorption coefficient and is taken as 2.2 cm^{-1} (80% linear transmittance), β is the two-photon absorption coefficient, and α_s is the effective scattering coefficient; g_s is a parameter that is independent of the laser intensity but depends on the size, shape, and concentration of the particles and wavelength of light, $\Delta\tilde{n}$ is the difference in the effective refractive indices of both linear and nonlinear components, Δn_0 is the difference in the linear refractive indices of gold nanoparticles and toluene, and Δn_2 is the difference in the nonlinear refractive indices of gold nanoparticles and toluene. Using the Runge−Kutta fourth-order method (37), the solution to the above equation can be obtained by integrating over the time and transverse space of the laser pulses. The β and Δn_2 values can then be determined as 9.7×10^{-11} cm/W and 9.5×10^{-12} cm^2/W, respectively, through a least-squares fit of the experimental data (by taking linear refractive indices of gold and toluene as 0.17 and 1.4963, respectively, at 780 nm wavelength).

In summary, here we report strong broad-band optical-limiting properties of oleylamine-capped gold nanoparticles

for both femtosecond and nanosecond laser pulses. The thresholds for the optical-limiting properties of the oleylamine-capped gold nanoparticles with 532 and 1064 nm laser pulses are lower than those of the CNT suspension, which is known as a benchmark optical limiter. Fluence- and angle-dependent scattering measurements confirm that the nonlinear scattering plays a very important role in the exceptional optical-limiting activity of oleylamine-capped gold nanoparticles at 532 nm with 7 ns pulses, at 1064 nm with 7 ns pulses, and at 780 nm with 300 fs pulses. Two-photon absorption also partially contributes to the observed optical-limiting effects for femtosecond laser pulses at 780 nm. These nanoparticles could be a good replacement for CNTs for optical-limiting applications.

Acknowledgment. The authors thank the Faculty of Science, National University of Singapore, for financial support (Grants R-143-000-341-112 and R-143-000-403-112).

Supporting Information Available: Experimental method for the synthesis of gold nanoparticles in water and their extinction spectra, TEM images and optical-limiting measurements with nanosecond laser pulses at 532 and 1064 nm and with femtosecond laser pulses at 780 nm, and *z*-scan measurement for pure toluene at 780 nm and 300 fs laser pulses. This material is available free of charge via the Internet at http://pubs.acs.org.

REFERENCES AND NOTES

(1) Chen, P.; Wu, X.; Sun, X.; Lin, J.; Ji, W.; Tan, K. L. *Phys. Rev. Lett.* **1999**, *82*, 2548.
(2) He, G. S.; Tan, L. S.; Zheng, Q.; Prasad, P. N. *Chem. Rev.* **2008**, *108*, 1245.
(3) Elim, H. I.; Yang, J.; Lee, J. Y.; Mi, J.; Ji, W. *Appl. Phys. Lett.* **2006**, *88*, 083107.
(4) Polavarapu, L.; Xu, Q. H.; Dhoni, M. S.; Ji, W. *Appl. Phys. Lett.* **2008**, *92*, 263110.
(5) Liu, Z. B.; Tian, J. G.; Guo, Z.; Ren, D. M.; Du, T.; Zheng, J. Y.; Chen, Y. S. *Adv. Mater.* **2008**, *20*, 511.
(6) Wang, J.; Blau, W. J. *J. Phys. Chem. C* **2008**, *112*, 2298.
(7) Mansour, K.; Soileau, M. J.; Vanstryland, E. W. *J. Opt. Soc. Am. B* **1992**, *9*, 1100.
(8) Chen, Y.; Fujitsuka, M.; O'Flaherty, S. M.; Hanack, M.; Ito, O.; Blau, W. J. *Adv. Mater.* **2003**, *15*, 899.
(9) Calvete, M.; Yang, G. Y.; Hanack, M. *Synth. Met.* **2004**, *141*, 231.
(10) Francois, L.; Mostafavi, M.; Belloni, J.; Delaire, J. A. *Phys. Chem. Chem. Phys.* **2001**, *3*, 4965.
(11) Ispasoiu, R. G.; Balogh, L.; Varnavski, O. P.; Tomalia, D. A.; Goodson, T. *J. Am. Chem. Soc.* **2000**, *122*, 11005.
(12) Pan, H.; Chen, W. Z.; Feng, Y. P.; Ji, W.; Lin, J. Y. *Appl. Phys. Lett.* **2006**, 88, 223106.
(13) Philip, R.; Kumar, G. R.; Sandhyarani, N.; Pradeep, T. *Phys. Rev. B* **2000**, *62*, 13160.
(14) Porel, S.; Venkatram, N.; Rao, D. N.; Radhakrishnan, T. P. *J. Nanosci. Nanotechnol.* **2007**, *7*, 1887.
(15) Sun, W. F.; Dai, Q.; Worden, J. G.; Huo, Q. *J. Phys. Chem. B* **2005**, *109*, 20854.
(16) Sun, Y. P.; Riggs, J. E.; Rollins, H. W.; Guduru, R. *J. Phys. Chem. B* **1999**, *103*, 77.
(17) Wang, G.; Sun, W. F. *J. Phys. Chem. B* **2006**, *110*, 20901.
(18) Qu, S. L.; Gao, Y. C.; Jiang, X. W.; Zeng, H. D.; Song, Y. L.; Qiu, H. R.; Zhu, C. S.; Hirao, K. *Opt. Commun.* **2003**, *224*, 321.
(19) Francois, L.; Mostafavi, M.; Belloni, J.; Delouis, J. F.; Delaire, J.; Feneyrou, P. *J. Phys. Chem. B* **2000**, *104*, 6133.
(20) Sinani, V. A.; Gheith, M. K.; Yaroslavov, A. A.; Rakhnyanskaya, A. A.; Sun, K.; Mamedov, A. A.; Wicksted, J. P.; Kotov, N. A. *J. Am. Chem. Soc.* **2005**, *127*, 3463.
(21) Ganeev, R. A.; Baba, M.; Ryasnyansky, A. I.; Suzuki, M.; Kuroda, H. *Opt. Commun.* **2004**, *240*, 437.
(22) Scalora, M.; Dowling, J. P.; Bowden, C. M.; Bloemer, M. J. *Phys. Rev. Lett.* **1994**, *73*, 1368.
(23) Nair, S. S.; Thomas, J.; Sandeep, C. S. S.; Anantharaman, M. R.; Philip, R. *Appl. Phys. Lett.* **2008**, *92*, 171908.
(24) Wang, J.; Hernandez, Y.; Lotya, M.; Coleman, J. N.; Blau, W. J. *Adv. Mater.* **2009**, *21*, 2430.
(25) Halder, A.; Ravishankar, N. *Adv. Mater.* **2007**, *19*, 1854.
(26) Lu, X. M.; Tnan, H. Y.; Korgel, B. A.; Xia, Y. N. *Chem.—Eur. J.* **2008**, *14*, 1584.
(27) He, G. S.; Yong, K. T.; Zheng, Q. D.; Sahoo, Y.; Baev, A.; Ryasnyanskiy, A. I.; Prasad, P. N. *Opt. Express* **2007**, *15*, 12818.
(28) Jain, P. K.; Qian, W.; El-Sayed, M. A. *J. Am. Chem. Soc.* **2006**, *128*, 2426.
(29) Melinger, J. S.; Kleiman, V. A.; McMorrow, D.; Grohn, F.; Bauer, B. J.; Amis, E. *J. Phys. Chem. A* **2003**, *107*, 3424.
(30) Polavarapu, L.; Xu, Q. H. *Nanotechnology* **2009**, *20*, 185606.
(31) Lee, Y. H.; Yan, Y. L.; Polavarapu, L.; Xu, Q. H. *Appl. Phys. Lett.* **2009**, *95*, 023105.
(32) Hartland, G. V. *Annu. Rev. Phys. Chem.* **2006**, *57*, 403.
(33) Farrer, R. A.; Butterfield, F. L.; Chen, V. W.; Fourkas, J. T. *Nano Lett.* **2005**, *5*, 1139.
(34) Eichelbaum, M.; Schmidt, B. E.; Ibrahim, H.; Rademann, K. *Nanotechnology* **2007**, *18*, 355702.
(35) Venkatram, N.; Rao, D. N.; Akundi, M. A. *Opt. Express* **2005**, *13*, 867.
(36) Joudrier, V.; Bourdon, P.; Hache, F.; Flytzanis, C. *Appl. Phys. B: Lasers Opt.* **1998**, *67*, 627.
(37) Butcher, J. C.; Cash, J. R.; Vanderhouwen, P. J. *J. Comput. Appl. Math.* **1993**, *45*, 1.

AM900442U